ACS APPLIED POLYMER MATERIALS

pubs.acs.org/acsapm Article

Block Copolymer Pressure-Sensitive Adhesives Derived from Fatty Acids and Triacetic Acid Lactone

Hussnain Sajjad, William B. Tolman,* and Theresa M. Reineke*

Cite This: https://dx.doi.org/10.1021/acsapm.0c00317 Read Online

ACCESS | Metrics & More | Article Recommendations | Supporting Information

ABSTRACT: A method for the development of ABA triblock copolymers for high-performance pressure-sensitive adhesives from the biorenewable chemicals lauryl acrylate and triacetic acid lactone (TAL) is presented. Lauryl acrylate, readily derived from vegetable oils, was polymerized via a reversible addition−fragmentation chain-transfer process to yield high-molecular-weight telechelic polymers. The synthesis of triblock copolymers was accomplished by subsequent chain extension with TAL, which is available from carbohydrates via the action of genetically modified yeast. The resulting triblock copolymers were found to exhibit excellent adhesion, with tunable peel forces up to 8 N cm^{-1} when a rosin ester-based tackifier was used. Tack forces up to 7 N cm^{-1} and no shear failure up to 100 h demonstrate the competitive performance of the potentially sustainable adhesives with commercial commodity products.

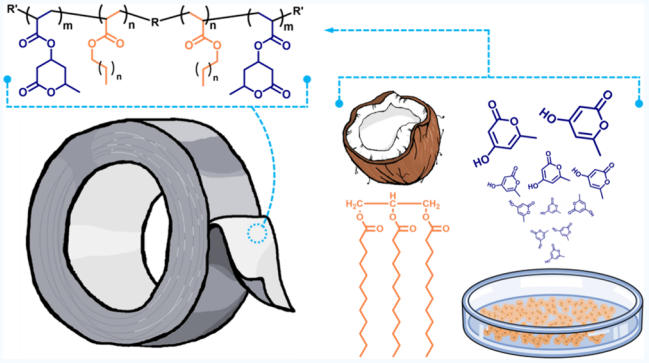

KEYWORDS: *triblock copolymers, pressure-sensitive adhesives, triacetic acid lactone (TAL), lauryl acrylate, sustainability, sustainable polymers, block polymer*

Downloaded via Laura Seifert on June 12, 2020 at 14:35:53 (UTC).
See https://pubs.acs.org/sharingguidelines for options on how to legitimately share published articles.

INTRODUCTION

Thermoplastic elastomers (TPEs) comprise an important class of reprocessable materials that have found use in a wide range of applications including pressure-sensitive adhesives (PSAs), footwear, electronics, and medical devices.[1,2] Petroleum-based triblock copolymers with an ABA architecture, such as poly(styrene-butadiene-styrene) (SBS) or poly(styrene-isoprene-styrene), have been traditionally used as TPEs. The ABA-type architecture, employing a "rubbery" midblock (B) and flanking "glassy" blocks (A), allows for molecular variation in composition, which influences the nanoscale structure of the material and ultimately dictates its application and use.[3,4] For example, immiscibility of the high T_g poly(styrene) domains with the low T_g poly(butadiene) domains in SBS triblock copolymers leads to phase-segregated nanostructures, which enhance the mechanical properties of the material.[3]

The use of finite, petroleum-based platform chemicals for the manufacturing of TPEs, however, is concerning from a sustainability and environmental viewpoint. Consequently, the development of soft materials from alternative, more sustainable sources is a major contemporary societal demand,[5−7] and researchers have maintained a focused effort into replacing the outer (A) and/or inner (B) blocks with biorenewable feedstocks. For example, poly(lactide) (PLA) has been used as a glassy component in TPEs with various lactones, alkenes, glycols, menthide, or ricinoleic acid serving as the rubbery component.[8−22] Although PLA is used as the glassy component, its relatively low glass-transition temperature (T_g) limits its utility in TPEs. Acrylic block copolymers, however, offer functional versatility (such as tunable T_g values) because of the ability to vary the pendant ester group. Notable examples in recent years have employed renewable terpene derivatives as replacements for the rubbery and glassy blocks in triblock copolymers for PSAs and elastomers.[23,24] In a similar fashion, we previously reported on the production of TPEs employing acrylic derivatives of glucose and isosorbide as replacements for the glassy, styrene-based endblocks in traditional TPEs.[25−28] Using reversible addition−fragmentation chain-transfer (RAFT) polymerization as a controlled polymerization technique,[29,30] *n*-butyl acrylate (nBA) was copolymerized with the acrylate-functionalized sugar derivatives to create triblock copolymers with an ABA-type architecture. Poly nBA has a low glass-transition temperature (−47 °C) and an entanglement molecular weight of 28 kDa[31,32] and is often used as a rubbery midblock in ABA-type polymers for PSA applications. Because the elastic modulus of an elastomer is related to the average molecular weight

Received: March 26, 2020
Accepted: May 14, 2020

© XXXX American Chemical Society

between entanglements, polymers with larger M_e values are favorable for PSAs owing to their inherently lower elastic modulus compared to traditional butadiene- or isoprene-based elastomers.[33] The adhesive and mechanical properties of the resultant ABA-triblock materials were comprehensively evaluated and shown to exhibit promising properties that depended on block identity, molecular weight, and tackifier presence. Another notable example similarly used RAFT polymerization to copolymerize nBA with acrylic derivatives of phenolic compounds obtained from the depolymerization of lignocellulosic biomass to create PSAs.[34] While these studies substituted the glassy component of acrylic-based TPEs, sustainability is difficult to attain because of the use of p(nBA) as the rubbery midblock.

Although it is feasible to derive nBA from bio-sourced *n*-butanol,[35] an arguably more attractive choice for the midblock in the context of this work is lauryl acrylate (LauAc). Lauryl alcohol can be directly obtained from the fatty acids of vegetable oils and is a major component of coconut and palm kernel oils.[36,37] In illustrative applications, lauryl acrylate and stearyl acrylate were copolymerized with styrene via RAFT polymerization to create elastomers with an ABA-type architecture.[37,38] As a consequence of the high entanglement molecular weights (M_e) of longer-chain alkyl acrylates, the resultant elastomers were weaker than the traditional SBS elastomers (i.e., exhibited lower stress and strain at break). PSAs of this architecture, however, benefit from the use of a base elastomer with a high entanglement molecular weight. We postulated that the higher M_e of p(LauAc) should yield an elastomer that exhibits a lower elastic modulus in comparison to p(nBa), a property that is desirable for instantaneous bonding of an adhesive to a substrate.

In addition to exploring alternatives for the midblock in ABA copolymers, we also sought to replace styrene with renewable feedstocks for use in synthesizing the glassy component in TPEs. We chose 4-hydroxy-6-methyl-2-pyrone [denoted as triacetic acid lactone (TAL)], which can be obtained synthetically from acetic acid[39−41] or through biological pathways in select microbes, which synthesize the compound as a secondary metabolite of glucose and other sugars.[42−44] Notably, ongoing research into the genetic bioengineering of *Escherichia coli* and *Saccharomyces cerevisiae* suggests that biologically synthesized TAL may be a viable feedstock.[45−50] Although TAL and its numerous derivatives have been studied for their efficacy as food preservatives, antimicrobials, pharmaceuticals, and so forth, its use as a renewable feedstock for polymer synthesis has yet to be explored in detail.[41,49,51] In a recent study, partial substitution of p(epichlorohydrin) with TAL via postpolymerization modification resulted in an apparent increase in the T_g of the material from −30 °C up to 70 °C depending on the degree of substitution.[49]

We hypothesized that TAL and its hydrogenated derivative could be readily substituted with acrylic groups and polymerized via controlled methods, resulting in a material with properties suitable for use as a glassy component in bio-sourced multiblock copolymer TPEs for PSA applications. In addition, we postulated that renewable rubbery blocks derived from vegetable oils can replace p(nBA) as the base elastomer. Herein, we report functionalization of TAL directly with acryloyl chloride, as well as the synthesis of a similarly substituted variant derived from hydrogenating TAL. Block copolymerization with lauryl acrylate as the rubbery midblock was performed to create a series of well-defined, high-molar-mass ABA acrylic triblock copolymers. Adhesion performance studies (peel adhesion, loop tack, and shear failure) revealed functional properties comparable to commercial PSAs. This work demonstrates a new strategy for the preparation of functional block copolymer PSAs from renewably sourced building blocks.

EXPERIMENTAL SECTION

Materials. 4-Hydroxy-6-methyl-2-pyrone ("TAL" "pyrone") was purchased from Oakwood Chemical and used without further purification. Pd/C (10 wt % loading) was purchased from Sigma-Aldrich and dried under vacuum prior to use. Acryloyl chloride, nBA, and lauryl acrylate were purchased from Sigma-Aldrich, passed through basic alumina to remove inhibitors, and stored at −30 °C until further use. The RAFT chain-transfer agent (CTA) [(3,5-bis(2-dodecylthiocarbonothioylthio-1-oxopropoxy)benzoic acid (BTCBA)] and 2,2′-azobis(2-methylpropionitrile) (AIBN) were purchased from Sigma-Aldrich and used as-received. The rosin ester tackifier (SYLVALITE RE-80HP) was from Arizona Chemical and used as-received.

Characterization. All reported ^{1}H NMR spectra were collected on a Bruker AVANCE III HD 500 MHz spectrometer in deuterated chloroform ($CDCl_3$), and chemical shifts are referenced to tetramethylsilane at 0.00 ppm. The spectra of all small molecules were collected at 22 °C with D1 = 1 s (16 scans), and the spectra of all polymers were collected at 22 °C with D1 = 10 s (64 scans). High-resolution mass spectrometry (HRMS) was performed using a Bruker BioTOF II in positive mode. Tetrahydrofuran (THF) size exclusion chromatography (SEC) was performed in uninhibited THF utilizing a Waters Styragel guard column and three consecutive Waters Styragel columns at a flow rate of 1 mL min^{-1} at 22 °C. The instrument was equipped with an Agilent 1260 Infinity liquid chromatograph coupled with a Wyatt Dawn Heleos II multiangle light scattering detector (18 angles from 10 to 160° and a 662.6 nm laser) and a Wyatt Optilab T-rEX refractive index detector. Dimethylformamide (DMF) SEC was performed in DMF with 0.05 M LiBr at a flow rate of 1.0 mL min^{-1} at 50 °C. The instrument was equipped with a Wyatt Dawn Heleos II multiangle light scattering detector (18 angles from 10 to 160° and a 662.6 nm laser) and a Wyatt Optilab T-rEx refractive index detector. The reported dn/dc values were calculated from the RI signal using a known sample concentration and assuming 100% mass recovery from the column and used for molar mass determination. Thermogravimetric analysis (TGA) was performed on a TA Instruments Q500 series at a heating rate of 10 °C min^{-1} under 60/40 nitrogen/oxygen flow. Differential scanning calorimetry (DSC) experiments were conducted with a TA Instruments Discovery DSC, using samples hermetically sealed in aluminum pans, at a heating/cooling rate of 10 °C min^{-1}. The reported $T_g/T_c/T_m$ values were from the second heating/cooling ramps. Adhesion and tensile testing was performed on a Shimadzu AGS-X tensile tester.

Hydrogenation of 4-Hydroxy-6-methyl-2-pyrone (TAL). Uninhibited THF was stirred over activated 3 Å molecular sieves for 24 h and filtered through a bed of Celite prior to use. A 300 mL high-pressure reactor vessel was charged with TAL (12.0 g, 95.1 mmol), Pd/C (1.2 g, 10% by mass), and 200 mL of THF. The reactor was sealed, first pressurized and depressurized with argon (3×) to remove O_2, then pressurized with gaseous H_2 to 100 psi, heated to 50 °C, and then pressurized to 500 psi. Over the next 48 h, the reactor vessel was periodically repressurized to 500 psi, after which time the vessel was cooled to room temperature and purged with argon to remove H_2. The reaction mixture was then filtered through a bed of Celite to remove the Pd/C. THF was removed under vacuum to afford 4-hydroxy-6-methyl-2-lactone ("lactone") (11.7 g, 95% isolated yield). ^{1}H NMR (400 MHz, chloroform-*d*): δ 4.44−4.29 (m, 1H), 4.25 (ddt, J = 9.3, 7.8, 5.7 Hz, 1H), 2.97 (s, 1H), 2.91−2.83 (m, 1H), 2.45 (ddd, J = 17.1, 7.8, 1.9 Hz, 1H), 2.28 (dddd, J = 13.8, 5.8, 3.1, 1.4 Hz, 1H), 1.63−1.52 (m, 1H), 1.41 (dd, J = 6.1, 1.8 Hz, 3H). ^{1}H NMR shifts reported here match the spectrum previously reported in ref 49.

https://dx.doi.org/10.1021/acsapm.0c00317
ACS Appl. Polym. Mater. XXXX, XXX, XXX−XXX

Synthesis of 4-Acrylate-6-methyl-2-pyrone (Acrylated-pyrone, AcPy). TAL (4-hydroxy-6-methyl-2-pyrone) (10.0 g, 79.3 mmol), acryloyl chloride (7.18 g, 79.3 mmol), and 100 mL of anhydrous CH_2Cl_2 were sequentially added to a dry 200 mL round-bottom flask. The flask was sealed with a rubber septum and submerged in an ice bath, and then, NEt_3 (10.1 mL, 7.29 g, 72.1 mmol) was added dropwise to the stirring solution. After 4 h, the precipitated NEt_3HCl salt was removed by filtration, and the filtrate was washed with 100 mL of a saturated sodium bicarbonate solution (×3) and once with 100 mL of brine. The organic layer was dried over magnesium sulfate, filtered, and concentrated under vacuum to yield a yellow liquid. The yellow liquid was loaded onto a silica column (2″ diameter × 1.5′ length), and a mixture of diethyl ether/hexanes (4:1) was used as the eluent. The desired compound elutes first from the column. The solvents were then removed under vacuum to afford AcPy (6.2 g, 43.6% isolated yield). ^{1}H NMR (500 MHz, chloroform-*d*): δ 6.62 (d, J = 17.2 Hz, 1H), 6.24 (dd, J = 17.2, 10.5 Hz, 1H), 6.11 (d, J = 10.1 Hz, 2H), 6.02 (d, J = 1.8 Hz, 1H), 2.28 (s, 3H). ^{13}C{^{1}H} NMR (126 MHz, chloroform-*d*): δ 163.67, 163.35, 163.03, 134.83, 126.68, 101.23, 101.07, 20.12. HRMS (ESI-TOF, m/z): calcd for $C_9H_8O_4Na^+$, 203.0315; observed, 203.0305.

Synthesis of 4-Acrylate-6-methyl-2-lactone (Acrylated-lactone, AcLa). Lactone (11.7 g, 89.9 mmol), acryloyl chloride (8.97 g, 99.1 mmol), and 100 mL of anhydrous CH_2Cl_2 were sequentially added to a dry 200 mL round-bottom flask. The flask was sealed with a rubber septum and submerged in an ice bath, and then, *N*,*N*-diisopropylethylamine (17.3 mL, 12.8 g, 99.1 mmol) was added dropwise to the stirring solution. After 2 h, CH_2Cl_2 was removed under vacuum to yield a dark orange oil. The oil was diluted with 5 mL of CH_2Cl_2 and loaded onto a silica column (5″ diameter × 1′ length), and neat diethyl ether was used as the eluent (note: excess acryloyl chloride elutes first and then the desired product. R_f = 0.35). The solvent was removed under vacuum to afford AcLa (11.0 g, 66.4% isolated yield). ^{1}H NMR (400 MHz, chloroform-*d*): δ 6.43 (dd, J = 17.3, 1.3 Hz, 1H), 6.10 (dd, J = 17.3, 10.5 Hz, 1H), 5.89 (dd, J = 10.4, 1.3 Hz, 1H), 5.29 (m, 1H), 4.47−4.37 (m, 1H), 2.96 (ddd, J = 17.2, 6.4, 1.0 Hz, 1H), 2.62 (dd, J = 17.3, 6.6 Hz, 1H), 2.43 (dddd, J = 14.0, 6.2, 2.9, 1.0 Hz, 1H), 1.67 (ddd, J = 14.1, 11.6, 8.6 Hz, 1H), 1.43 (d, J = 6.3 Hz, 3H). ^{13}C{^{1}H} NMR (126 MHz, chloroform-*d*): δ 169.53, 165.18, 131.93, 127.81, 73.08, 66.01, 36.23, 35.56, 21.17. HRMS (ESI-TOF, m/z): calcd for $C_9H_{12}O_4Na^+$, 207.0628; observed, 207.0621.

Synthesis of Poly(acrylated-lactone) (p(AcLa)) via Free Radical Polymerization. Acrylated-lactone (0.200 g, 1.09 mmol), AIBN (1.78 mg, 10.8 μmol) (from a dilute stock solution), and 5 mL of acetonitrile were added to a vacuum flask. The flask was sealed and degassed by four consecutive freeze−pump−thaw cycles and then submerged in a preheated oil bath at 70 °C. After stirring vigorously for 18 h, the flask was immediately submerged in liquid nitrogen until frozen and opened to the atmosphere. After thawing the solution at room temperature, the polymer was precipitated in cold H_2O and washed repeatedly with methanol until pure (monitored via ^{1}H NMR). The polymer was then dried in a vacuum oven at 60 °C for 24 h (50% conversion via ^{1}H NMR spectroscopy, 0.100 g, 50% isolated yield). ^{1}H NMR (400 MHz, chloroform-*d*): δ 5.26 (s, 1H), 4.45 (s, 1H), 2.28 (s, 1H), 2.61 (s, 1H), 2.42 (s, 1H), 2.30 (s, 1H), 1.86 (s, 2H), 1.69 (s, 1H), 1.45 (s, 3H). M_n(p(AcLa)) = 30 kg mol^{-1}, $Đ$ = 1.60.

Synthesis of Poly(*n*-butyl acrylate) via RAFT (CTA−p(nBA)−CTA). The synthesis of the macro-CTA was performed following literature procedures.[24−26] AIBN (5.12 mg, 0.031 mmol), BTCBA (128 mg, 0.156 mmol), and nBA (10.0 g, 78.0 mmol) were added to a dry 50 mL vacuum flask. The flask was sealed and degassed by four freeze−pump−thaw cycles and then submerged in a preheated oil bath at 70 °C. After stirring vigorously for 2 h, the flask was immediately submerged in liquid nitrogen and opened to the atmosphere. CH_2Cl_2 (10 mL) was added to the flask, and the polymer was precipitated in 200 mL of cold methanol. After allowing the contents to settle for 1 h, methanol was decanted, and 200 mL of additional cold methanol was added. The process was repeated twice, and then the purified CTA−p(nBA)−CTA polymer was dried in a vacuum oven at 60 °C for 18 h (84% conversion via ^{1}H NMR spectroscopy, 8.14 g, 81.0% isolated yield). ^{1}H NMR (500 MHz, chloroform-*d*): δ 4.04 (dq, J = 18.6, 10.1 Hz, 2H), 2.40−2.22 (m, 1H), 1.93 (m, 2H), 1.63 (m, 2H), 1.39 (m, 2H), 0.95 (t, J = 7.5 Hz, 3H). M_n(CTA−p(nBA)−CTA) = 55 kg mol^{-1}, $Đ$ = 1.05, dn/dc = 0.066.

Synthesis of CTA−p(AcLa)−p(nBA)−p(AcLa)−CTA. An illustrative example is provided. CTA−p(nBA)−CTA (1.0 g, 0.018 mmol), acrylated-lactone (AcLa) (0.335 g, 1.81 mmol), AIBN (0.299 mg, 1.82 μmol) (from a dilute stock solution), and 10 mL of DMF were added to a vacuum flask. The flask was sealed and degassed by four consecutive freeze−pump−thaw cycles and then submerged in a preheated oil bath at 70 °C. After stirring vigorously for 24 h, the flask was immediately submerged in liquid nitrogen and opened to the atmosphere. The polymer was precipitated in cold H_2O and washed repeatedly with methanol until DMF and the unreacted monomer were removed (monitored via ^{1}H NMR). The precipitates were then dried in a vacuum oven at 60 °C for 24 h. ^{1}H NMR (500 MHz, chloroform-*d*): δ 5.26 (s, 1H), 4.44 (s, 1H), 4.05 (m, 2H), 2.94 (s, 1H), 2.59 (s, 1H), 2.50−2.22 (m, 4H), 1.92 (s, 2H), 1.79−1.54 (m, 4H), 1.50−1.33 (m, 5H), 0.95 (t, J = 7.6 Hz, 3H).

Synthesis of Poly(lauryl acrylate) via RAFT (CTA−p(LauAc)−CTA). The synthesis of macro-CTA was performed following modified literature procedures.[24−26] AIBN (0.27 mg, 1.64 μmol from stock solution), BTCBA (6.8 mg, 8.36 μmol), and lauryl acrylate (2.0 g, 8.32 mmol) were added to a dry 50 mL vacuum flask. The flask was sealed and degassed by four freeze−pump−thaw cycles and then submerged in a preheated oil bath at 70 °C. After stirring vigorously for 3 h, the flask was immediately submerged in liquid nitrogen and opened to the atmosphere. $CHCl_3$ (10 mL) was added to the flask, and the polymer was precipitated in 200 mL of cold methanol. After allowing the contents to settle for 1 h, methanol was decanted, and 200 mL of additional cold methanol was added. The process was repeated twice and then the purified CTA−p(LauAc)−CTA polymer was dried in a vacuum oven at 60 °C for 18 h (88% conversion via ^{1}H NMR spectroscopy, 1.60 g, 80.0% isolated yield). ^{1}H NMR (500 MHz, chloroform-*d*): δ 4.01 (s, 2H), 2.31 (m, 1H), 1.91 (s, 2H), 1.70−1.54 (m, 8H), 1.31 (m, J = 19.0 Hz, 16H), 0.90 (t, J = 6.8 Hz, 3H). M_n(CTA−p(LaulAc)−CTA) = 230 kg mol^{-1}, $Đ$ = 1.16, dn/dc = 0.067.

Synthesis of CTA−p(AcLa)−p(LauAc)−p(AcLa)−CTA. An illustrative example is provided. CTA−p(LauAc)−CTA (0.5 g, 2.17 μmol), acrylated-lactone (AcLa) (0.12 g, 0.65 mmol), AIBN (71.4 μg, 0.43 μmol) (from a dilute stock solution), and 5 mL of $CHCl_3$ were added to a vacuum flask. The flask was sealed and degassed by four consecutive freeze−pump−thaw cycles and then submerged in a preheated oil bath at 70 °C. After stirring vigorously for 24 h, the flask was immediately submerged in liquid nitrogen and opened to the atmosphere. The polymer was precipitated in cold methanol and washed repeatedly with methanol until the unreacted monomer was removed (monitored via ^{1}H NMR). The precipitates were then dried in a vacuum oven at 60 °C for 24 h. ^{1}H NMR (500 MHz, chloroform-*d*): δ 5.24 (s, 1H), 4.44 (s, 1H), 4.07 (s, 2H), 2.95 (s, 1H), 2.60 (s, 1H), 2.52−2.19 (m, 3H), 1.94 (s, 2H), 1.62 (s, 11H), 1.46 (s, 3H), 1.30 (m, 16H), 0.90 (t, J = 6.8 Hz, 3H).

Dynamic Mechanical Analysis. Dynamic mechanical analysis (DMA) of poly(LauAc) (M_n = 300 kDa) was performed at 5 °C within the linear viscoelastic regime. An oscillatory stress was applied to sample between two 25 mm steel plates, and the sinusoidal stress response was measured. The resultant complex modulus was decoupled into the in-phase/elastic (G') and out-of-phase/viscous (G'') moduli. The loss tangent (tan δ), which is the ratio of the viscous modulus G'' to the elastic modulus G', was also calculated. The plateau in the storage modulus versus angular frequency curve (26,460 Pa), corresponding to a minimum in tan δ, was used to calculate the entanglement molecular weight (M_e) of poly(LauAc) as 66 kDa.

Adhesion Testing. Samples for PSA evaluations were prepared by dissolving the polymer or polymer/tackifier blend in THF or $CHCl_3$

https://dx.doi.org/10.1021/acsapm.0c00317
ACS Appl. Polym. Mater. XXXX, XXX, XXX−XXX

to produce 30% solid content solution (example: 100 mg of polymer or 70 mg of polymer/30 mg of tackifier in 265 μL THF). The solution was then solvent-cast onto a 50 μm thick sheet of polyethylene terephthalate (PET) films using a standard laboratory drawdown rod to target a coat weight of 25 gsm. The films were allowed to dry under ambient conditions for 24 h and then cut into 1 cm wide strips for adhesion testing.

180° Peel Adhesion (PSTC-101 Adhesion Test Method). A 1 cm wide strip of the polymer-coated PET film was adhered, using a 500 g roller, to a dry stainless steel plate that was cleaned with acetone prior to the test. The PET film was then peeled from the stainless steel plate using a Shimadzu AGX-X tensile tester at a peel rate of 305 mm min^{-1}. The peel force was recorded as the maximum force measured during the test, and the reported average and standard deviation values were acquired from five replicates.

Loop Tack (PSTC-16 Adhesion Test Method). A 1 cm wide strip of the polymer-coated PET film was formed into a tear-drop-shaped loop and mounted onto the upper grip of the tensile tester. The loop was then lowered onto a dry stainless steel plate that was cleaned with acetone prior to the test to give a contact area of 1 cm × 1 cm. The tack force was recorded as the maximum force measured while raising the upper grip at a rate of 305 mm min^{-1}, and the reported average and standard deviation values were acquired from five replicates.

Shear Adhesion (PSTC-107 Adhesion Test Method). A 2.54 cm × 2.54 cm strip of the polymer-coated PET film was adhered, using a 500 g roller, to a dry stainless steel plate that was cleaned with acetone prior to the test. The steel plate was held at a 2° angle relative to a vertical plane, and a 1 kg weight was suspended from the test strip. The time to adhesive failure was recorded for three samples.

RESULTS AND DISCUSSION

Initial efforts focused on targeting high-molecular-weight poly(lauryl acrylate) (p(LauAc)) for testing as a suitable midblock in an ABA triblock copolymer. Despite the advantage of using an elastomer with a high M_e as discussed above, appreciable peel adhesion values for triblock-based PSAs are only obtainable if the molecular weight of the rubbery midblock is at least 2−3 times the entanglement molecular weight of the polymer (i.e., the elastomer is "loosely" entangled).[52] RAFT polymerization of nBA using a bifunctional CTA was previously introduced by our group as a means to synthesize a living, chain-extendable rubbery midblock for an acrylic-based system.[26−28] Using a similar RAFT polymerization method with a commercially available difunctional CTA (BTCBA), we synthesized high-molecular-weight p(LauAc) with narrow dispersities (M_n = 300 kDa, $Đ$ = 1.19) while retaining the living nature of the polymer chain for chain extension with a glassy block (Scheme 1, see Figure S1 for ^{1}H NMR spectrum). The TGA analysis of the p(LauAc) macro-CTA showed good thermal stability with 5% weight loss occurring at ∼330 °C (Figure S2). The DSC thermogram displays T_m = 2 °C, T_c = −5 °C, and no discernible T_g feature (Figure S3). The thermal features seen in the thermogram of p(LauAc) correspond to the crystallization and melting events of the pendant alkyl chains.[53−55]

Scheme 1. Synthesis of p(Lauryl acrylate) via RAFT Polymerization

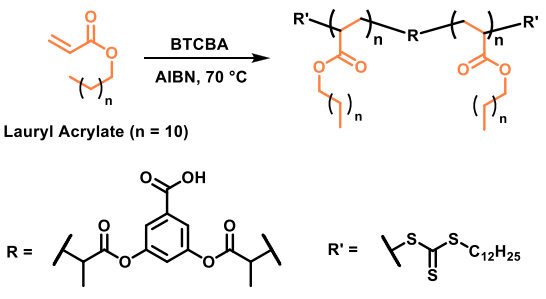

To validate that p(LauAc) is minimally entangled at the synthesized molecular weights, DMA was performed to calculate M_e, which had not been reported to date. The entanglement molecular weight was calculated using the moduli versus frequency plot shown in Figure 1 in conjunction with eq 1[56]

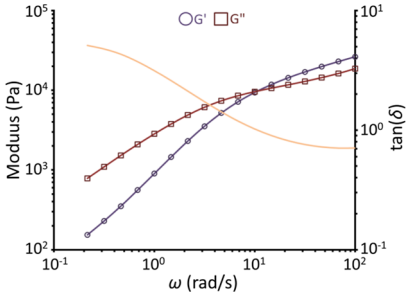

Figure 1. Plot of elastic (G') and loss (G'') moduli as a function of angular frequency at 5 °C of p(LauAc) with M_n = 300 kDa and $Đ$ = 1.19.

$$M_e = \frac{4}{5}\frac{\rho RT}{G_N^0} \quad (1)$$

where G_N^0 is the plateau modulus determined from oscillatory shear experiments, ρ is the density of the polymer (taken as 0.94 g/mL at 21 °C from the literature),[37] R is the gas constant, and T is the temperature at which the rheological experiments were conducted (5 °C). We note that although the reference temperature differs from the temperature at which the density measurement was performed, the difference in density of p(LauAc) between the two temperatures is expected to be negligible. Using the minimum of tan δ, a ratio of the loss to elastic moduli, as a reference point, the plateau modulus was determined to be 26,500 Pa, and the M_e of p(LauAc) was calculated to be 70 kDa. Therefore, polymers above approximately 210 kDa (i.e., ∼3 × M_e) are expected to be minimally entangled. A M_e value for poly(laurylmethacrylate) was reported to be 225 kDa based on rheological measurements on a sample with M_n = 82 kDa.[57] However, it is uncertain if the tested sample was suitably entangled in order to gather meaningful data for an accurate calculation.

We then sought to design efficient methods to create acrylic variants of TAL through two routes for polymerization into block polymer architectures (Scheme 2). Catalytic hydrogenation of TAL using Pd/C afforded the reduced lactone derivative (Figure S4).[51] The transformation approached near-quantitative yields under the given conditions after 2−3 days, depending on the scale. The lengthy reaction time toward complete hydrogenation is attributed to an internal keto−enol tautomerism, largely in favor of the keto-form, which is established following partial reduction of the pyrone ring (Scheme S1, Figure S5). Esterification of the hydroxyl substituents on both the pyrone and lactone rings with acryloyl chloride yielded 4-acrylate-6-methyl-2-pyrone (AcPy,

https://dx.doi.org/10.1021/acsapm.0c00317
ACS Appl. Polym. Mater. XXXX, XXX, XXX−XXX

Scheme 2. Syntheses of Acrylated-Pyrone (AcPy) and Acrylated-Lactone (AcLa)

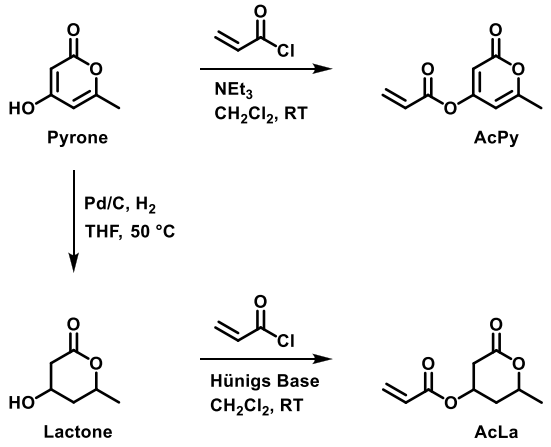

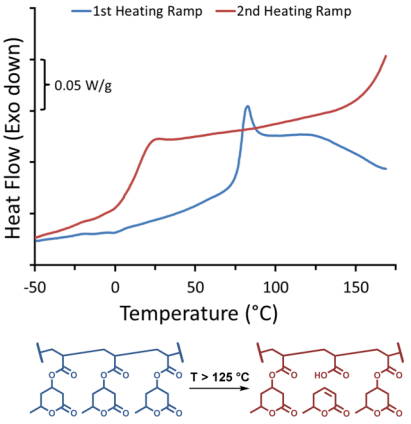

Figure 2. DSC thermograms of p(AcLa) from −50 to 170 °C taken on the first and second ramps of heating at 10°C min^{-1}. The synthetic scheme shown depicts the chemical change of the polymer at temperatures above 125 °C. The ^{1}H NMR spectrum of the ejected small molecule can be found in the Supporting Information (Figure S9).

Figures S6 and S7) and 4-acrylate-6-methyl-2-lactone (AcLa, Figures S8 and S9), respectively.

Prior to block copolymerization with p(LauAc), attempts toward the free radical and RAFT polymerizations of AcPy were carried out with azobis(isobutyronitrile) (AIBN) and various CTAs at 70 °C in DMF to establish reactivity and kinetics. Aliquots taken from the reaction mixture over time were analyzed by ^{1}H NMR spectroscopy, and the results indicated that no appreciable polymerization had occurred. In contrast, the free radical polymerization of AcLa under similar reaction conditions yielded p(AcLa) (Figure S10), reaching equilibrium at 88% conversion (^{1}H NMR spectroscopy). We speculate that the observed difference in reactivity between AcPy and AcLa toward radical polymerizations may be attributed to the alkene bonds of the pyrone ring, which can react with propagating radicals and lead to chain termination events.

The purified p(AcLa) homopolymer was analyzed by SEC in DMF with multiangle laser light scattering (SEC-MALLS) to determine a number-average molar mass (M_n) of 30 kg mol^{-1} and a dispersity ($Đ$) of 1.60 (Figure S11). TGA showed a thermal degradation temperature (T_d, 5 wt % loss) of 197 °C (Figure S12). Because degradation of polyacrylic backbones typically occurs at ∼300−350 °C following a random chain scission mechanism, the relatively lower observed T_d of p(AcLa) is likely due to the decomposition of the pendant lactone rings.[58,59] DSC analysis of the homopolymer, scanning to a maximum temperature limit of 170 °C, initially indicated a T_g of 84 °C (Figure 2). This relatively high T_g of p(AcLa) suggests that it can be used as a "glassy" component in a triblock copolymer system. Intriguingly, the DSC thermogram exhibited an exothermic feature beginning at 125 °C during the first temperature sweep; the second heating ramp in the experiment then showed a shift of the T_g value of the homopolymer to lower temperatures (∼23 °C in Figure 2). Both the exothermic feature and the observed shift in T_g between consecutive heating ramps were not observed if the DSC experiment was conducted to a maximum temperature limit of 110 °C (Figure S13). The soluble fraction of a sample of p(AcLa) subjected to temperatures above 125 °C was analyzed via ^{1}H NMR spectroscopy. The results indicated the presence of an unsaturated derivative of TAL (Figure S14), which is presumably ejected from the polymer backbone at elevated temperatures.[51,60] A change in the polymer sequence (i.e., interspersed acrylic acid moieties along the backbone of the polymer) and the presence of a small molecule within the polymer matrix are likely responsible for the observed shift in T_g shown in Figure 2. Nevertheless, because the formulated adhesives in this work are stable up to 125 °C, and only change chemically upon exposure to higher temperatures, processing temperatures of ∼100 °C (i.e., above the T_g of both blocks) would be unlikely to interfere with treatment. Additionally, because most of the commodity PSAs are typically used at room temperature (tape, sticky notes, etc.), the chemical change observed at elevated temperatures will not limit user-end applicability.

We then used a controlled radical polymerization strategy to prepare a family of triblock copolymers (Scheme 3).[61−63] In addition to testing p(LauAc) as the base elastomer, nBA was also polymerized in accordance with previous methods.[26,27,34] A molecular weight of 55 kDa for the p(nBA) midblock was targeted to allow for direct comparisons among the various PSAs, which have used p(nBA) of the same molecular weight as that of the base elastomer and different acrylic derivatives as the glassy endblocks. RAFT polymerization of nBA was performed in the bulk with AIBN and BTCBA at 70 °C to afford the living macro-CTA (see Figure S15 for ^{1}H NMR). The number-average molar mass, analyzed via THF SEC-MALLS, and the measured thermal data (T_d and T_g) of this rubbery midblock were in agreement with the values previously reported for this synthetic procedure (Table 1, Figures S16 and S17).[26,27] Lauryl acrylate was polymerized to target molecular weights such that the elastomer is minimally entangled (∼3 × M_e) and therefore has a low elastic modulus, which is desirable for bonding of the adhesive to a given substrate. The molecular weights of the glassy p(AcLa) endblocks were varied to examine the effect of higher hard block weight percentages on the adhesive performance of the PSAs.

Subsequent chain extension of the p(nBA) and p(LauAc) macro-CTAs with AcLa afforded the desired triblock copolymers. Successful chain extension was validated by observation of peaks corresponding to p(AcLa) in the ^{1}H NMR spectra (Figures S18 and S19) accompanied by a clear shift of the SEC traces to lower retention times when compared to the macro-CTAs (Figures S20−S22). The

https://dx.doi.org/10.1021/acsapm.0c00317
ACS Appl. Polym. Mater. XXXX, XXX, XXX−XXX

Scheme 3. Synthesis of p(AcLa)−p(nBA)−p(AcLa) and p(AcLa)−p(LauAc)−p(AcLa) Triblock Copolymers via RAFT Polymerization

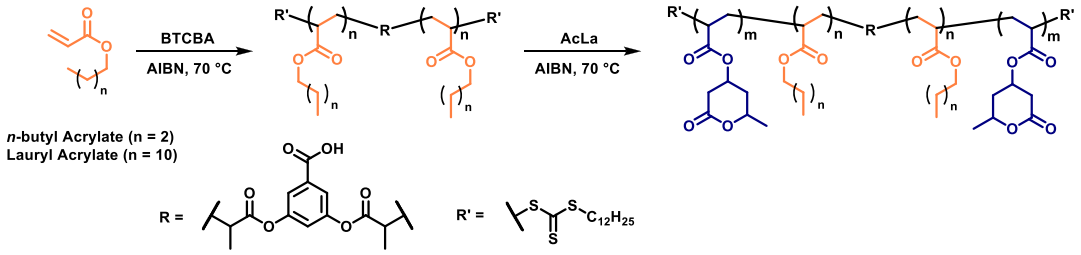

Table 1. Data Summary of the p(nBA) and p(LauAc) Macro-CTAs and Their Corresponding Chain-Extended Triblock Copolymers

polymer	sample code[a]	M_n[b] (kDa)	$Đ$[c]	hard block[d] (wt %)	T_d[e] (°C)	T_g[f] (°C)
p(nBA)		55	1.04		327	−47
p(AcLa)−p(nBA)−p(AcLa)	**P1**	2-55-2	1.13	5	286	−47
p(AcLa)−p(nBA)−p(AcLa)	**P2**	4-55-4	1.14	13	203	−47
p(AcLa)−p(nBA)−p(AcLa)	**P3**	7-55-7	1.16	20	200	−47, 84
p(AcLa)−p(nBA)−p(AcLa)	**P4**	10-55-10	1.14	27	198	−47, 84
p(LauAc)		230	1.16		336	
p(AcLa)−p(LauAc)−p(AcLa)	**P5**	10-230-10	1.29	8	210	
p(AcLa)−p(LauAc)−p(AcLa)	**P6**	15-230-15	1.25	12	203	84
p(LauAc)		300	1.19		336	
p(AcLa)−p(LauAc)−p(AcLa)	**P7**	9-300-9	1.36	6	220	

[a]p(nBA) was chain-extended to synthesize **P1−P4**, and p(LauAc) was chain-extended to synthesize **P5−P7**. [b]Number-average molar mass as determined through SEC. [c]Dispersity as determined through SEC. [d]AcLa content relative to total molecular weight. [e]Decomposition temperature corresponding to 5% weight loss as determined by TGA. [f]Observable glass-transition temperature(s) determined by DSC.

presence of a shoulder in the SEC traces at lower retention times is likely due to the formation of multiblock polymers stemming from termination-by-combination events. By adjusting the molar ratio of macro-CTA to AcLa in the reaction mixture, variable weight percentages of hard block content within the resultant triblock copolymers were attained (Table 1). The TGA profiles of the triblock copolymers (**P1−P7**) show two distinct features at 190 and 350 °C, corresponding to the decomposition of the pendant lactone rings and the acrylate backbone, respectively (Figures S23−S29). While the glass-transition temperature of the p(nBA) midblock can be clearly seen in the DSC thermograms of **P1−P4** (Figure 3), the T_g feature of the p(AcLa) blocks is only well defined in **P3** and **P4**, which have longer endblock lengths. The DSC thermograms of **P5−P7** (Figures S30−S32, respectively) show

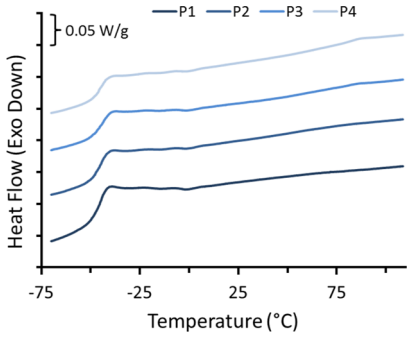

Figure 3. DSC thermograms of the triblock copolymers **P1−P4** at a heating rate of 10 °C·min^{-1} taken on the second heating cycle. The thermogram shows the T_g of the p(nBA) midblock to be −47 °C in all samples but a discernable feature corresponding to the T_g of the p(AcLa) endblocks at 84 °C only for **P3** and **P4**.

the T_m and T_c features of the dodecyl alkyl chains, but a discernable T_g peak for the p(AcLa) segments is only seen in **P6**, which also contains the highest weight fraction of the hard blocks. This observation has been reported for other triblock copolymers with a relatively low hard block content and is likely a result of the shorter p(AcLa) segments,[26,27,34] which ultimately translates to imperceptible heat exchange in the calorimetry experiment. Furthermore, a match of both the p(nBA) and p(AcLa) T_g values in the triblock copolymers to those of their homopolymers suggests that the two blocks are immiscible.[64]

To evaluate the materials as PSAs and understand how the ratio of glassy block affects their properties, samples for adhesion testing were prepared by casting solutions of the polymers onto a sheet of PET film (see the Supporting Information for details). The adhesive capabilities of thin films of the triblock copolymers with and without added ester-based tackifier were evaluated by pressure-sensitive tape council (PSTC) standard methods. The samples of triblock copolymers were mixed with an appropriate amount of tackifier, and the adhesive properties of the polymer and polymer/tackifier blends were evaluated and compared by a 180° peel test (PSTC-101) to assess adherence, a loop tack bonding test (PSTC-16) to measure tackiness (instantaneous bonding capability), and a static shear strength test (PSTC-107) to measure resistance to shear failure under an applied force. Another important factor in evaluating these PSAs is the mode of failure, which is qualitatively reported as "cohesive" or "adhesive". Cohesive failure is a result of failure within the adhesive layer, which leaves behind residue on the surface, while adhesive failure occurs at the interfacial boundary. Either mode may be acceptable depending on the desired application of the adhesive, with cohesive failure being more favorable for

https://dx.doi.org/10.1021/acsapm.0c00317
ACS Appl. Polym. Mater. XXXX, XXX, XXX−XXX

permanent PSAs and adhesive failure sought for removable PSAs.[16,26,33,65,66] Blending of an appropriate tackifier was carried out in order to dilute entanglements of the midblock and effectively lower the elastic modulus of the material, allowing for tunable adhesive values under controlled test conditions.[33,67] DSC measurements of **P1** and **P2** with added SYLVALITE 80HP rosin ester (a renewable resin manufactured by Arizona Chemicals) showed an increase in the T_g of the p(nBA) midblock relative to the homopolymer (from −48 to −26 °C, Figures S33 and S34), suggesting successful integration of the tackifier within the midblock.[68] A similar experiment with the p(LauAc)-based triblock copolymers did not produce a discernable T_g feature in the DSC thermograms. Maximum values of peel adhesion were obtained with 30 wt % of tackifier added to the nBA-based polymers and 40 wt % of tackifier added to the LauAc-based polymers. Incorporation of greater amounts of tackifier (e.g., 60 wt %) led to a reduction in tack. This observation has similarly been seen with other block copolymers[22,68,69] and is explained by the apparent increase in the T_g of the midblock with increasing tackifier content, ultimately diminishing the tackiness. The results of the adhesion tests for the triblock copolymers are summarized in Figure 4 and Table 2.

By varying the tackifier content, the peel adhesion values of the p(nBA)-based polymers can be tuned in the range of 2−6 N cm^{-1}, which are comparable to commercial commodity products such as Duct tape, Scotch tape, and so forth.[28,34]

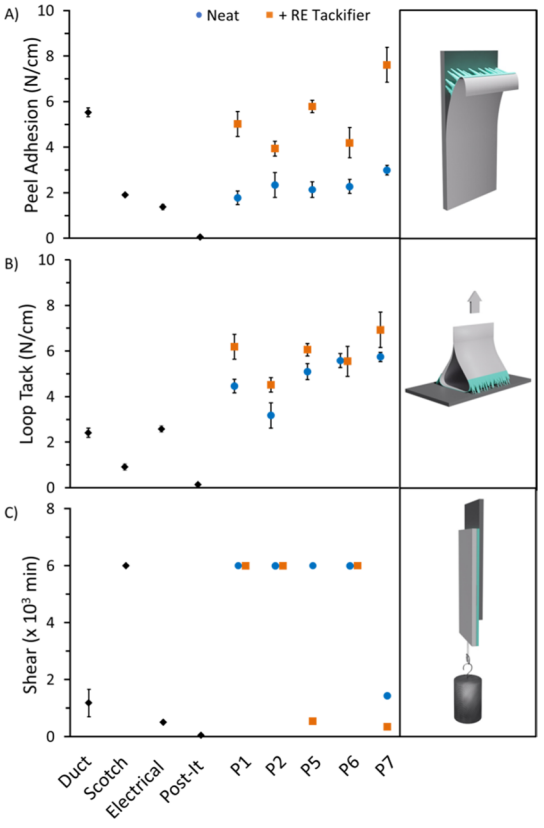

Figure 4. Adhesive performance of p(AcLa)−p(nBA)−p(AcLa) (**P1** and **P2**) and p(AcLa)−p(LauAc)−p(AcLa) (**P5**−**P7**) via (a) 180° peel, (b) loop tack, and (c) static shear tests compared to commercial product values (black diamonds) reported in ref 51. The authors acknowledge John Beumer for creating the 3-D model images of the adhesion tests depicted in the figure.

Cohesive failure was observed during the peel adhesion test of **P1**, while adhesive failure was observed for **P2**. The difference in the failure modes between **P1** and **P2** likely stems from the degree of endblock length, whereby longer lengths of the hard blocks translate to stronger intermolecular interactions within the glassy domains. These interactions result in stronger cohesive forces within the adhesive layer, which leads to adhesive failure. Measured loop tack forces were in the range of 3−6 N cm^{-1}, also comparable to commercial products. Notably, the adhesives demonstrated excellent shear resistance under an applied static load. All formulations examined for adhesion, regardless of the hard block weight percentage or tackifier content, did not fail for the duration of the testing period (100 h at room temperature). A comparison of these results to previous studies which have also used p(nBA) as the rubbery component for triblock-based PSAs[26,27,34] shows that peel adhesion forces are within the same 2−4 N cm^{-1} range (when the tackifier is disregarded), despite the fact that different acrylic derivatives were used as the glassy component in each study. These results suggest that the adhesive forces in triblock PSA systems are predominately influenced by the base elastomer. That is, if p(nBA) is "loosely" entangled and contributes 80−90% of the copolymer by weight, the measured adhesion forces will be similar regardless of the glassy component used. The materials obtained from **P3** and **P4**, which incorporated greater amounts of the glassy component in the polymers, exhibited negligible tack and thus could not be tested for adhesion.

Samples of **P5**−**P7** were also blended with the rosin ester tackifier, and the polymers and polymer/tackifier blends were evaluated as previously described. The results of the adhesion tests are summarized in Figure 4. Peel adhesion values are tunable in the range of 2−8 N cm^{-1} depending on tackifier content. Adhesive failure mode was observed only for **P6**, which has the greatest hard block content in this series. The measured peel adhesion forces of the neat p(LauAc)-based polymers were in the same range as the neat p(nBA)-based polymers (2−4 N cm^{-1}), proving that longer alkyl acrylates can effectively be used as the base elastomer for PSAs as long as the higher M_e can be overcome. The measured loop tack forces were in the range of 5−8 N cm^{-1}, consistently greater than those measured for the PSAs which use p(nBA) as the rubbery midblock with similar hard block lengths. This observation is likely a consequence of the lower elastic modulus of p(LauAc) than that of p(nBA), resulting in a "tackier" material which adheres to the substrate more quickly. The shear test results indicated that the p(LauAc) series of polymers performed worse than the p(nBA) series. Only **P6**, which has the greatest hard block weight fraction, demonstrated resistance to shear failure on par with the p(nBA) series. Addition of tackifier to **P5** and **P7**, which theoretically lowers the elastic modulus of the elastomer, resulted in greater peel adhesion and loop tack forces but led to a reduction in shear resistance. The spread of adhesion/tack forces and shear failure shows that the formulations of these sustainably sourced acrylic adhesives can be modified in a systematic manner to target a specific application (i.e., permanent vs removable PSAs) and are competitive in performance to commodity products on the market today. Additionally, in contrast to other biorenewable PSAs which use a polyester-based rubbery midblock,[11,12,16,22] this acrylic-based system is shown to exhibit good adhesion both with and without tackifier additives because of the lower elastic modulus; however, polyester-based

https://dx.doi.org/10.1021/acsapm.0c00317
ACS Appl. Polym. Mater. XXXX, XXX, XXX−XXX

Table 2. Adhesion Testing Summary of the p(nBa) (P1 and P2) and p(LauAc) (P5−P7) Triblock Copolymers

sample code	M_n (kDa) (hard block wt %)	peel adhesion[b] (N cm^{-1})	loop tack[c] (N cm^{-1})	shear[d] (min)
P1	2-55-2(7)	1.78 ± 0.30	4.46 ± 0.64	>6000
		5.02 ± 0.55[a]	6.19 ± 0.95[a]	>6000[a]
P2	4-55-4(13)	2.34 ± 0.55	3.17 ± 0.85	>6000
		3.94 ± 0.32[a]	4.52 ± 0.82[a]	>6000[a]
P5	10-230-10(8)	2.14 ± 0.35	5.10 ± 0.64	>6000
		5.79 ± 0.27[a]	6.06 ± 0.33[a]	548 ± 19[a]
P6	15-230-15(12)	2.28 ± 0.31	5.58 ± 0.59	>6000
		4.20 ± 0.66[a]	5.55 ± 0.15[a]	>6000[a]
P7	9-300-9(6)	2.99 ± 0.20	5.74 ± 0.37	1430 ± 26
		7.62 ± 0.77[a]	6.93 ± 1.59[a]	343 ± 71[a]

[a]Adhesion values for the polymer blended with a rosin ester resin as a tackifier. [b]180° peel test using a stainless steel plate as the adherend, test method: PSTC-101. [c]Loop tack test to a stainless steel plate, test method: PSTC-16. [d]Static shear adhesion to a stainless steel plate using 2.54 cm × 2.54 cm films and a 1 kg load, test method: PSTC-107.

PSAs still maintain the distinct advantage of better degradability over their acrylic counterparts.

CONCLUSIONS

In summary, we have reported the synthesis and study of new sustainable acrylic triblock copolymers for PSAs. Lauryl acrylate was employed as the rubbery midblock in place of commonly used nBA in an effort to improve upon the renewability aspect of the adhesives. Furthermore, TAL, an emerging platform chemical, was modified and subsequently copolymerized via RAFT polymerization to develop an acrylate-based system suitable for PSAs. The synthesized polymers were of high molecular weights and narrow dispersities, specific component ratios were targeted, and the adhesives demonstrated similar performance to commercial products. The intrinsically lower elastic modulus of p(LauAc) promoted excellent adhesion and tack capabilities of the resultant triblock copolymers. Use of high T_g p(AcLa) as the glassy component in the triblock copolymers enhanced the physical properties of the adhesives (e.g., high shear forces and adhesive failure mode), albeit with limited thermal stability at temperatures above 125 °C, which could be explored to trigger thermally responsive release properties. We demonstrate through this robust strategy that it is indeed possible to utilize renewable, long-chained alkyl-acrylates with high M_e in conjunction with biologically accessible TAL to realize a fully sustainable system for high-performance PSA applications.

ASSOCIATED CONTENT

Supporting Information

The Supporting Information is available free of charge at https://pubs.acs.org/doi/10.1021/acsapm.0c00317.

Materials, characterization, synthetic protocols, DMA, and adhesion testing; ^{1}H NMR spectra of monomers and polymers; SEC traces, TGAs, and DSC thermograms of macro-CTAs and polymers; and adhesion testing of **P1**, **P2**, **P5**, **P6**, and **P7** with and without a tackifier (PDF)

AUTHOR INFORMATION

Corresponding Authors

William B. Tolman − *Department of Chemistry, Washington University in St. Louis, St. Louis, Missouri 63130-4899, United States;* orcid.org/0000-0002-2243-6409; Email: wbtolman@wustl.edu

Theresa M. Reineke − *Department of Chemistry and Center for Sustainable Polymers, University of Minnesota, Minneapolis, Minnesota 55455-0431, United States;* orcid.org/0000-0001-7020-3450; Email: treineke@umn.edu

Author

Hussnain Sajjad − *Department of Chemistry and Center for Sustainable Polymers, University of Minnesota, Minneapolis, Minnesota 55455-0431, United States;* orcid.org/0000-0003-1283-5884

Complete contact information is available at: https://pubs.acs.org/10.1021/acsapm.0c00317

Notes

The authors declare no competing financial interest.

ACKNOWLEDGMENTS

This work was supported by the National Science Foundation under the Center for Sustainable Polymers (CHE-1901635). The authors acknowledge John Beumer for creating the 3-D model images of the adhesion tests in Figure 4.

REFERENCES

(1) Legge, N. R.; Holden, G.; Schroeder, H. E. *Thermoplastic Elastomers: A Comprehensive Review*; Hanser Publishers: Munich, 1987.

(2) Holden, G. Thermoplastic Elastomers and Their Applications. In *Applied Polymer Science: 21st Century*; Craver, C. D., Carraher, C. E., Jr., Eds.; Elsevier: Oxford, 2007; pp 231−256.

(3) Bates, F. S.; Fredrickson, G. H. Block Copolymers-Designer Soft Materials. *Phys. Today* **1999**, *52*, 32−38.

(4) Nagpal, U.; Detcheverry, F. A.; Nealey, P. F.; De Pablo, J. J. Morphologies of Linear Triblock Copolymers from Monte Carlo Simulations. *Macromolecules* **2011**, *44*, 5490−5497.

(5) Weisz, P. B. Basic Choices and Constraints on Long-Term Energy Supplies. *Phys. Today* **2004**, *57*, 47−52.

(6) Zhu, Y.; Romain, C.; Williams, C. K. Sustainable Polymers from Renewable Resources. *Nature* **2016**, *540*, 354−362.

(7) Wang, Z.; Yuan, L.; Tang, C. Sustainable Elastomers from Renewable Biomass. *Acc. Chem. Res.* **2017**, *50*, 1762−1773.

(8) Watts, A.; Kurokawa, N.; Hillmyer, M. A. Strong, Resilient, and Sustainable Aliphatic Polyester Thermoplastic Elastomers. *Biomacromolecules* **2017**, *18*, 1845−1854.

(9) Qian, H.; Bei, J.; Wang, S. Synthesis, Characterization and Degradation of ABA Block Copolymer of L-Lactide and ε-Caprolactone. *Polym. Degrad. Stab.* **2000**, *68*, 423−429.

(10) Cohn, D.; Hotovely-Salomon, A. Biodegradable Multiblock PEO/PLA Thermoplastic Elastomers: Molecular Design and Properties. *Polymer* **2005**, *46*, 2068−2075.
(11) Hillmyer, M. A.; Tolman, W. B. Aliphatic Polyester Block Polymers: Renewable, Degradable, and Sustainable. *Acc. Chem. Res.* **2014**, *47*, 2390−2396.
(12) Lee, S.; Yuk, J. S.; Park, H.; Kim, Y.-W.; Shin, J. Multiblock Thermoplastic Elastomers Derived from Biodiesel, Poly(Propylene Glycol), and L-Lactide. *ACS Sustainable Chem. Eng.* **2017**, *5*, 8148−8160.
(13) Frick, E. M.; Zalusky, A. S.; Hillmyer, M. A. Characterization of Polylactide-b-Polyisoprene-b-Polylactide Thermoplastic Elastomers. *Biomacromolecules* **2003**, *4*, 216−223.
(14) Lebarbé, T.; Ibarboure, E.; Gadenne, B.; Alfos, C.; Cramail, H. Fully Bio-Based Poly(L-Lactide)-b-Poly(Ricinoleic Acid)-b-Poly(L-Lactide) Triblock Copolyesters: Investigation of Solid-State Morphology and Thermo-Mechanical Properties. *Polym. Chem.* **2013**, *4*, 3357−3369.
(15) Lee, S.; Lee, K.; Jang, J.; Choung, J. S.; Choi, W. J.; Kim, G.-J.; Kim, Y.-W.; Shin, J. Sustainable poly(ε-Decalactone)−poly(L-Lactide) Multiarm Star Copolymer Architectures for Thermoplastic Elastomers with Fixed Molar Mass and Block Ratio. *Polymer* **2017**, *112*, 306−317.
(16) Lee, S.; Lee, K.; Kim, Y.-W.; Shin, J. Preparation and Characterization of a Renewable Pressure-Sensitive Adhesive System Derived from ε-Decalactone, L -Lactide, Epoxidized Soybean Oil, and Rosin Ester. *ACS Sustainable Chem. Eng.* **2015**, *3*, 2309−2320.
(17) Schneiderman, D. K.; Hill, E. M.; Martello, M. T.; Hillmyer, M. A. Poly(Lactide)-Block-Poly(ε-Caprolactone-Co-ε-Decalactone)-Block-Poly(Lactide) Copolymer Elastomers. *Polym. Chem.* **2015**, *6*, 3641−3651.
(18) Schneiderman, D. K.; Hillmyer, M. A. Aliphatic Polyester Block Polymer Design. *Macromolecules* **2016**, *49*, 2419−2428.
(19) Schneiderman, D. K.; Gilmer, C.; Wentzel, M. T.; Martello, M. T.; Kubo, T.; Wissinger, J. E. Sustainable Polymers in the Organic Chemistry Laboratory: Synthesis and Characterization of a Renewable Polymer from δ-Decalactone and l-Lactide. *J. Chem. Educ.* **2014**, *91*, 131−135.
(20) Arrington, K. J.; Waugh, J. B.; Radzinski, S. C.; Matson, J. B. Photo- and Biodegradable Thermoplastic Elastomers: Combining Ketone-Containing Polybutadiene with Polylactide Using Ring-Opening Polymerization and Ring-Opening Metathesis Polymerization. *Macromolecules* **2017**, *50*, 4180−4187.
(21) Wanamaker, C. L.; O'Leary, L. E.; Lynd, N. A.; Hillmyer, M. A.; Tolman, W. B. Renewable-Resource Thermoplastic Elastomers Based on Polylactide and Polymenthide. *Biomacromolecules* **2007**, *8*, 3634−3640.
(22) Shin, J.; Martello, M. T.; Shrestha, M.; Wissinger, J. E.; Tolman, W. B.; Hillmyer, M. A. Pressure-Sensitive Adhesives from Renewable Triblock Copolymers. *Macromolecules* **2011**, *44*, 87−94.
(23) Noppalit, S.; Simula, A.; Ballard, N.; Callies, X.; Asua, J. M.; Billon, L. Renewable Terpene Derivative as a Biosourced Elastomeric Building Block in the Design of Functional Acrylic Copolymers. *Biomacromolecules* **2019**, *20*, 2241−2251.
(24) Noppalit, S.; Simula, A.; Billon, L.; Asua, J. M. Paving the Way to Sustainable Waterborne Pressure-Sensitive Adhesives Using Terpene-Based Triblock Copolymers. *ACS Sustainable Chem. Eng.* **2019**, *7*, 17990−17998.
(25) Gallagher, J. J.; Hillmyer, M. A.; Reineke, T. M. Isosorbide-Based Polymethacrylates. *ACS Sustainable Chem. Eng.* **2015**, *3*, 662−667.
(26) Gallagher, J. J.; Hillmyer, M. A.; Reineke, T. M. Acrylic Triblock Copolymers Incorporating Isosorbide for Pressure Sensitive Adhesives. *ACS Sustainable Chem. Eng.* **2016**, *4*, 3379−3387.
(27) Nasiri, M.; Reineke, T. M. Sustainable Glucose-Based Block Copolymers Exhibit Elastomeric and Adhesive Behavior. *Polym. Chem.* **2016**, *7*, 5233−5240.
(28) Nasiri, M.; Saxon, D. J.; Reineke, T. M. Enhanced Mechanical and Adhesion Properties in Sustainable Triblock Copolymers via Non-Covalent Interactions. *Macromolecules* **2018**, *51*, 2456−2465.
(29) Chiefari, J.; Chong, Y. K.; Ercole, F.; Krstina, J.; Jeffery, J.; Le, T. P. T.; Mayadunne, R. T. A.; Meijs, G. F.; Moad, C. L.; Moad, G.; Rizzardo, E.; Thang, S. H. Living Free-Radical Polymerization by Reversible Addition - Fragmentation Chain Transfer: The RAFT Process. *Macromolecules* **1998**, *31*, 5559−5562.
(30) Perrier, S. 50th Anniversary Perspective: RAFT Polymerization - A User Guide. *Macromolecules* **2017**, *50*, 7433−7447.
(31) Tong, J.-D.; Jerôme, R. Dependence of the Ultimate Tensile Strength of Thermoplastic Elastomers of the Triblock Type on the Molecular Weight between Chain Entanglements of the Central Block. *Macromolecules* **2000**, *33*, 1479−1481.
(32) Tong, J. D.; Jerôme, R. Synthesis of poly(methyl methacrylate)-b-poly(n-butyl acrylate)-b- poly(methyl methacrylate) Triblocks and Their Potential as Thermoplastic Elastomers. *Polymer* **2000**, *41*, 2499−2510.
(33) Creton, C. Pressure-Sensitive Adhesives: An Introductory Course. *MRS Bull.* **2003**, *28*, 434−439.
(34) Wang, S.; Shuai, L.; Saha, B.; Vlachos, D. G.; Epps, T. H. From Tree to Tape: Direct Synthesis of Pressure Sensitive Adhesives from Depolymerized Raw Lignocellulosic Biomass. *ACS Cent. Sci.* **2018**, *4*, 701−708.
(35) Vendamme, R.; Schüwer, N.; Eevers, W. Recent Synthetic Approaches and Emerging Bio-Inspired Strategies for the Development of Sustainable Pressure-Sensitive Adhesives Derived from Renewable Building Blocks. *J. Appl. Polym. Sci.* **2014**, *131*, 40669.
(36) Noweck, K.; Grafahend, W. Fatty Alcohols. *Ullman's Encyclopedia of Industrial Chemistry*; John Wiley & Sons, Inc., 2006; Vol. *14*, pp 114−141.
(37) Wang, S.; Vajjala Kesava, S.; Gomez, E. D.; Robertson, M. L. Sustainable Thermoplastic Elastomers Derived from Fatty Acids. *Macromolecules* **2013**, *46*, 7202−7212.
(38) Ding, W.; Robertson, M. L. Sustainable Thermoplastic Elastomers with a Transient Network. *Eur. Polym. J.* **2019**, *113*, 411−423.
(39) Collie, J. N. LVI.-The lactone of triacetic acid. *J. Chem. Soc., Trans.* **1891**, *59*, 607−617.
(40) Obydennov, D. L.; El-Tantawy, A. I.; Sosnovskikh, V. Y. Triacetic Acid Lactone as a Bioprivileged Molecule in Organic Synthesis. *Mendeleev Commun.* **2019**, *29*, 1−10.
(41) Shanks, B. H.; Keeling, P. L. Bioprivileged Molecules: Creating Value from Biomass. *Green Chem.* **2017**, *19*, 3177−3185.
(42) Xie, D.; Shao, Z.; Achkar, J.; Zha, W.; Frost, J. W.; Zhao, H. Microbial Synthesis of Triacetic Acid Lactone. *Biotechnol. Bioeng.* **2006**, *93*, 727−736.
(43) Goel, A.; Ram, V. J. Natural and Synthetic 2H-Pyran-2-Ones and Their Versatility in Organic Synthesis. *Tetrahedron* **2009**, *65*, 7865−7913.
(44) Eckermann, S.; Schröder, G.; Schmidt, J.; Strack, D.; Edrada, R. A.; Helariutta, Y.; Elomaa, P.; Kotilainen, M.; Kilpeläinen, I.; Proksch, P.; Teeri, T. H.; Schröder, J. New Pathway to Polyketides in Plants. *Nature* **1998**, *396*, 387−390.
(45) Tang, S.-Y.; Qian, S.; Akinterinwa, O.; Frei, C. S.; Gredell, J. A.; Cirino, P. C. Screening for Enhanced Triacetic Acid Lactone Production by Recombinant Escherichia Coli Expressing a Designed Triacetic Acid Lactone Reporter. *J. Am. Chem. Soc.* **2013**, *135*, 10099−10103.
(46) Cardenas, J.; Da Silva, N. A. Metabolic Engineering of Saccharomyces Cerevisiae for the Production of Triacetic Acid Lactone. *Metab. Eng.* **2014**, *25*, 194−203.
(47) Saunders, L. P.; Bowman, M. J.; Mertens, J. A.; Da Silva, N. A.; Hector, R. E. Triacetic Acid Lactone Production in Industrial Saccharomyces Yeast Strains. *J. Ind. Microbiol. Biotechnol.* **2015**, *42*, 711−721.
(48) Yu, J.; Landberg, J.; Shavarebi, F.; Bilanchone, V.; Okerlund, A.; Wanninayake, U.; Zhao, L.; Kraus, G.; Sandmeyer, S. Bioengineering

https://dx.doi.org/10.1021/acsapm.0c00317
ACS Appl. Polym. Mater. XXXX, XXX, XXX−XXX

Triacetic Acid Lactone Production in Yarrowia Lipolytica for Pogostone Synthesis. *Biotechnol. Bioeng.* **2018**, *115*, 2383−2388.
(49) Markham, K. A.; Palmer, C. M.; Chwatko, M.; Wagner, J. M.; Murray, C.; Vazquez, S.; Swaminathan, A.; Chakravarty, I.; Lynd, N. A.; Alper, H. S. Rewiring Yarrowia Lipolytica toward Triacetic Acid Lactone for Materials Generation. *Proc. Natl. Acad. Sci. U.S.A.* **2018**, *115*, 2096−2101.
(50) Li, Y.; Qian, S.; Dunn, R.; Cirino, P. C. Engineering Escherichia Coli to Increase Triacetic Acid Lactone (TAL) Production Using an Optimized TAL Sensor-Reporter System. *J. Ind. Microbiol. Biotechnol.* **2018**, *45*, 789−793.
(51) Chia, M.; Schwartz, T. J.; Shanks, B. H.; Dumesic, J. A. Triacetic Acid Lactone as a Potential Biorenewable Platform Chemical. *Green Chem.* **2012**, *14*, 1850−1853.
(52) Abbott, S. *Adhesion Science, Principles and Practice*; DEStech Publications: Lancaster, 2015.
(53) Rehberg, C. E.; Fisher, C. H. Preparation and Properties of the N-Alkyl Acrylates. *J. Am. Chem. Soc.* **1944**, *66*, 1203−1207.
(54) Mogri, Z.; Paul, D. R. Membrane Formation Techniques for Gas Permeation Measurements for Side-Chain Crystalline Polymers. *J. Membr. Sci.* **2000**, *175*, 253−265.
(55) O'Leary, K.; Paul, D. R. Copolymers of Poly(n-Alkyl Acrylates): Synthesis, Characterization, and Monomer Reactivity Ratios. *Polymer* **2004**, *19*, 6575−6585.
(56) Liu, C.; He, J.; Ruymbeke, E. v.; Keunings, R.; Bailly, C. Evaluation of Different Methods for the Determination of the Plateau Modulus and the Entanglement Molecular Weight. *Polymer* **2006**, *47*, 4461−4479.
(57) Chatterjee, D. P.; Mandal, B. M. Triblock Thermoplastic Elastomers with Poly(Lauryl Methacrylate) as the Center Block and Poly (Methyl Methacrylate) or Poly(Tert-Butyl Methacrylate) as End Blocks. Morphology and Thermomechanical Properties. *Macromolecules* **2006**, *39*, 9192−9200.
(58) Mahalik, J. P.; Madras, G. Effect of the Alkyl Group Substituents on the Thermal and Enzymatic Degradation of Poly(n-Alkyl Acrylates). *Ind. Eng. Chem. Res.* **2005**, *44*, 4171−4177.
(59) Witkowski, A.; Stec, A. A.; Hull, T. R. Thermal Decomposition of Polymeric Materials. In *SFPE Handbook of Fire Protection Engineering, 5*; Gottuk, D., Hall, J. R., Jr., Harada, K., Kuligowski, E., Puchovsky, M., Torero, J., Watts, J. M., Jr., Weiczorek, C., Eds.; Springer: New York, 2016; Vol. *1*, pp 167−254.
(60) Chia, M.; Haider, M. A.; Pollock, G.; Kraus, G. A.; Neurock, M.; Dumesic, J. A. Mechanistic Insights into Ring-Opening and Decarboxylation of 2-Pyrones in Liquid Water and Tetrahydrofuran. *J. Am. Chem. Soc.* **2013**, *135*, 5699−5708.
(61) Moad, G.; Rizzardo, E.; Thang, S. H. Living Radical Polymerization by the RAFT Process. *Aust. J. Chem.* **2005**, *58*, 379−410.
(62) Barner-Kowollik, C.; Perrier, S. The Future of Reversible Addition Fragmentation Chain Transfer Polymerization. *J. Polym. Sci., Part A: Polym. Chem.* **2008**, *46*, 5715−5723.
(63) Keddie, D. J. Guide to the Synthesis of Block Copolymers Using Reversible-Addition Fragmentation Chain Transfer (RAFT) Polymerization. *Chem. Soc. Rev.* **2014**, *43*, 496−505.
(64) Fox, T. G.; Flory, P. J. Second-Order Transition Temperatures and Related Properties of Polystyrene. I. Influence of Molecular Weight. *J. Appl. Phys.* **1950**, *21*, 581−591.
(65) Chang, E. P. Viscoelastic Properties of Pressure-Sensitive Adhesives. *J. Adhes.* **1997**, *60*, 233−248.
(66) Benedek, I. *Pressure-Sensitive Adhesives and Applications*, 2nd ed., Revised and Expanded; Marcel Dekker: New York, 2004.
(67) Daoulas, K. C.; Theodorou, D. N.; Roos, A.; Creton, C. Experimental and Self-Consistent-Field Theoretical Study of Styrene Block Copolymer Self-Adhesive Materials. *Macromolecules* **2004**, *37*, 5093−5109.
(68) Nakajima, N.; Babrowicz, R.; Harrell, E. R. Rheology, Composition, and Peel-mechanism of Block Copolymer−Tackifier-based Pressure Sensitive Adhesives. *J. Appl. Polym. Sci.* **1992**, *44*, 1437−1456.
(69) Brown, K.; Hooker, J. C.; Creton, C. Micromechanisms of Tack of Soft Adhesives Based on Styrenic Block Copolymers. *Macromol. Mater. Eng.* **2002**, *287*, 163−179.

https://dx.doi.org/10.1021/acsapm.0c00317
ACS Appl. Polym. Mater. XXXX, XXX, XXX−XXX